

# Convection Theory and Sub-photospheric Stratification

David Arnett<sup>1</sup>, Casey Meakin<sup>1</sup>, and Patrick A. Young<sup>2,1</sup>  
 darnett@as.arizona.edu, casey.meakin@gmail.com, patrick.young.1@asu.edu

## ABSTRACT

As a step toward a complete theoretical integration of 3D compressible hydrodynamic simulations into stellar evolution, convection at the surface and sub-surface layers of the Sun is re-examined, from a restricted point of view, in the language of mixing-length theory (MLT). Requiring that MLT use a hydrodynamically realistic dissipation length gives a new constraint on solar models. While the stellar structure which results is similar to that obtained by YREC (Guenther, Demarque, Kim & Pinsonneault 1992; Bahcall & Pinsonneault 2004) and Garching models (Schlatter, Weiss & Ludwig 1997), the theoretical picture differs. A new quantitative connection is made between macro-turbulence, micro-turbulence, and the convective velocity scale at the photosphere, which has finite values. The “geometric parameter” in MLT is found to correspond more reasonably with the size of the strong downward plumes which drive convection (Stein & Nordlund 1998), and thus has a physical interpretation even in MLT. Use of 3D simulations of both adiabatic convection and stellar atmospheres will allow the determination of the dissipation length and the geometric parameter (i.e., the entropy jump), *with no astronomical calibration*.

A physically realistic treatment of convection in stellar evolution will require additional modifications beyond MLT, including effects of kinetic energy flux, entrainment (the most dramatic difference from MLT found by Meakin & Arnett (2007b)), rotation, and magnetic fields (Balbus & Hawley 1998; Balbus 2008).

*Subject headings:* stars: evolution - stars: hydrodynamics - convection - Sun: photosphere - white dwarfs - atmospheres:3D - Binaries: eclipsing

## 1. Introduction

Recent simulations of three-dimensional compressible convection and their theoretical analysis (Meakin & Arnett 2007b; Arnett, Meakin, & Young 2009) have shown that the interpretation of mixing-length theory (MLT), as currently

used in stellar evolution (Böhm-Vitense 1958; Cox 1968; Clayton 1983; Hansen & Kawaler 1994; Kippenhahn & Weigert 1990) is flawed. This mixing length  $\ell$  is parameterized as  $\alpha_{ML} \ell / H_P$ , where  $H_P$  is the local pressure scale height, and  $\alpha_{ML}$  is adjusted to reproduce the radius of the present-day Sun. However, instead of being an adjustable parameter, the mixing length is found to correspond to the dissipation length  $\ell_d$  of the turbulence (Kolmogorov 1941, 1962), and de-

<sup>1</sup>Steward Observatory, University of Arizona, 933 N. Cherry Avenue, Tucson AZ 85721

<sup>2</sup>School of Earth and Space Exploration, Arizona State University, Tempe, AZ

terminated by the size of the largest eddies (Meakin & Arnett 2007b; Arnett, Meakin, & Young 2009). From our own simulations (Meakin & Arnett 2009) and those of others we find a robust tendency for the dissipation length to be

$$\ell_d \approx \min(\ell_{CZ}, 4H_P), \quad (1)$$

where  $\ell_{CZ}$  is the depth of the convection zone. For shallow convection zones, the dissipation length is limited by the depth of the convective region, and seems to approach a limiting value of  $\ell_d \approx 4H_P$  for deep convection zones.

If  $\alpha_{ML}$  is fixed, other parameters in MLT, which are generally left fixed by historical convention, may be adjusted to compensate (e.g., (Tassoul, Fontaine, & Winget 1990; Salaris & Cassisi 2008)). The most significant of these parameters is the geometric factor<sup>1</sup>, which adjusts the rate at which radiation limits the degree of entropy excess in the super-adiabatic region (SAR). For simplicity we use  $g_{ML}$  to denote the geometric factor in units of the value used in conventional MLT (see Appendix for details). If we identify the geometric parameter as a measure of the size of the SAR, we remove the last free parameter in MLT. Although MLT is an incomplete theory, it does serve as a useful "language" to explain some of the changes implied by 3D simulations.

The mixing length theory itself (Vitense 1953; Böhm-Vitense 1958), if used consistently, does capture many (but not all) aspects of turbulent convection. However, a real replacement for MLT will provide a global solution and relax the local connection between the superadiabatic gradient and the enthalpy flux, so that regions of the convective zone can be subadiabatic, as observed in simulations.

In order to establish a "baseline" from which to compare new effects demanded by

numerical simulations and by laboratory experiment (e.g., fluctuations, non-locality, and entrainment), the framework of the standard solar model (Bahcall, Serenelli, & Pinsonneault 2004) is examined with respect to modification of some aspects of convection. In this paper we show that the addition of dynamically realistic values of mixing length and geometric factor give some interesting insights into the nature of the average stratification of the Sun just below the photosphere. In Section 2 we construct a series of solar models with  $\alpha_{ML}$ — $g_{ML}$  pairs, to delineate their properties. The notion of a "standard solar model" derives from the work of John Bahcall and collaborators, and is summarized in Bahcall (1989). It represents what is probably the most carefully tested aspect of the theory of stellar evolution. In Section 3 we compare our models to standard results using the Yale Rotational Evolution Code (Guenther, Demarque, Kim & Pinsonneault 1992; Bahcall & Pinsonneault 2004), and the Garching code (see Schlattl (1996); Schlattl, Weiss & Ludwig (1997)). In Section 4 we compare the outer layers of our models to the 3D atmospheres of Nordlund and Stein (Asplund, et al. 2005), semi-empirical models of the solar atmosphere (Fontenla et al. 2006), and re-examine the question of convective velocities at the photosphere. In Section 5 we summarize the implications of this work.

## 2. Solar Models

### 2.1. Hydrodynamically-consistent MLT Parameters

Tassoul, Fontaine, & Winget (1990) have defined the parameters in MLT in a concise way: they define three parameters  $a$ ,  $b$ , and  $c$  in terms of an adjustable mixing length  $\ell$ . In the notation of Arnett, Meakin, & Young (2009),  $\Delta\nabla = \nabla - \nabla_e$ , so we have

$$a = v_c^2 H_P / \ell^2 g \beta_T \Delta\nabla, \quad (2)$$

<sup>1</sup>This is essentially the  $c$  factor of Tassoul, Fontaine, & Winget (1990).

TABLE 1  
MIXING LENGTH PARAMETERS<sup>a</sup>

MLT choice	$a$	$b$	$c$	$\ell$
BV58 <sup>b</sup>	0.125	0.5	24	free parameter
ML2 <sup>c</sup>	1	2	16	free parameter
AMY <sup>d</sup>	$\approx 0.1$	0.256	$24/g_{ML}$ <sup>e</sup>	$\min(4H_P, \ell_{CZ})$

<sup>a</sup>As defined in Tassoul, Fontaine, & Winget (1990).

<sup>b</sup>Böhm-Vitense (1958); this is ML1.

<sup>c</sup>Tassoul, Fontaine, & Winget (1990); Salaris & Cassisi (2008)

<sup>d</sup>Arnett, Meakin, & Young (2009), and this paper.

<sup>e</sup> $g_{ML} = (\ell/\sqrt{3}r_b)^2$ , where  $r_b$  is the radius of a blob just contained inside the SAR.

$$b = F_c H_P / \rho v_c C_P T \ell \Delta \nabla, \quad (3)$$

and

$$c = C_P \rho^2 \ell v_c \kappa (\nabla_e - \nabla_a) / \sigma T^3 \Delta \nabla \quad (4)$$

Table 1 gives standard values for the mixing length parameters in the formulation of Tassoul, Fontaine, & Winget (1990). The first two entries are the standard "flavor" due to Böhm-Vitense (1958), and the ML2 flavor of Tassoul, Fontaine, & Winget (1990). In both cases the values of  $a$ ,  $b$ , and  $c$  are fixed and the mixing length  $\ell$  adjusted to reproduce the solar radius of the present day Sun. The third line presents the values of these parameters as estimated from 3D simulations (Meakin & Arnett 2007b; Arnett, Meakin, & Young 2009). Two striking differences are apparent: (1) the mixing length is not an arbitrary constant. For deep convection zones (like the Sun which has  $\ell_{CZ} = 20H_P$ ) the mixing length (dissipation length) approaches  $4H_P$ . (2) the "c" parameter is intimately related to the geometric factor, and we assume to the thickness of the superadiabatic layer. Both the "a" and "b" parameter are fixed at

the values for adiabatic turbulent convection (Arnett, Meakin, & Young 2009), leaving  $c = 24/g_{ML}$  as the remaining free parameter. Note that the flavors BV58 (ML1) and ML2 both differ from those suggested by the simulations.

Even though there are additional effects shown in 3D turbulent simulations which are not contained in MLT, it is useful to examine those changes which can be captured with a standard stellar evolution code. If the value of  $\alpha_{ML} = \ell/H_P$  is fixed, which of these parameters is to be varied in MLT to get an acceptable solar model? The only parameter sufficient to the task is the "geometric parameter" (i.e.,  $c$  or  $g_{ML}$ ). A simple way to examine the effects of the geometric parameter is to vary its value relative to the value used in conventional MLT; we denote this scaled value by  $g_{ML}$  (see the Appendix below). We relate this factor to the size of the SAR by  $g_{ML} = (\ell_d/\sqrt{3}r_b)^2$ , where the "blob diameter"  $2r_b$  is the thickness of the SAR. MLT results if we set  $g_{ML} = 1$ ; this identifies the SAR with the superadiabatic "element" of Kippenhahn & Weigert (1990), p. 50. In

MLT, the "blob" is assumed to have a dimension fixed by the mixing length. This is inconsistent with 3D atmosphere simulations (Stein & Nordlund 1998)) and solar models (Guenther, Demarque, Kim & Pinsonneault (1992); Schlattl, Weiss & Ludwig (1997) and below), which show that the superadiabatic region is narrow, less than a pressure scale height thick. MLT has *two* characteristic lengths, one of which is ignored by forcing the geometric parameter length scale to be the same as the mixing length (turbulent dissipation length). We will allow the "blob" size to differ from the mixing length in order to vary  $g_{ML}$ .

For theoretical clarity we will apply radiative diffusion theory consistently up to the photosphere. While radiation transfer theory is more accurate than radiative diffusion, it is more cumbersome, and itself is affected by the convection model used (VandenBerg, et al. 2008). After we understand the convection problem better, this approach can be extended by a more sophisticated multi-dimensional treatment of radiative transfer in the outer regions. Comparison to 3D hydrodynamic atmospheres (e.g., Stein & Nordlund (1998); Nordlund & Stein (2000)) can test the validity of this approach.

## 2.2. Standard Input Physics

These computations were done using the TYCHO stellar evolution code (revision 12; version control by SVN). Opacities were from Iglesias & Rogers (1996) and Alexander & Ferguson (1994) with Grevesse & Sauval (1998) abundances. The OPAL-EOS (Rodgers, Swenson & Iglesias (1996) equation of state was used over the range of conditions relevant here. The Timmes & Swesty (2000) equation of state is automatically used for higher densities and temperatures, with a smooth interpolation across the joining region. The formulation of MLT is from Kippenhahn & Weigert

(1990), with the modifications via the dimensionless geometric factor  $g_{ML}$  as given in the Appendix;  $g_{ML} \equiv 1$  gives conventional MLT. We stress that convection is treated in exactly the same way, with the same parameters, in the interior and in the envelope (VandenBerg, et al. 2008). Diffusion was treated with the Thoul subroutine (see Thoul, Bahcall, & Loeb (1994)); radiative levitation (Michaud et al. 2004) was ignored. The nuclear reactions were solved in a 177 isotope network using ReacLib (Rauscher & Thielemann 2000); weak screening rates were incorporated as in John Bahcall's `exportenergy.f` program. The changes in metallicity due to nuclear reactions and to diffusion were taken into account by interpolation in both the opacity and the equation of state tables. The same equation of state and opacity tables are used in the interior and the atmosphere.

## 2.3. Modified MLT Models

We examine the solar models resulting from several choices of the mixing length, each constructed by varying the geometric factor  $g_{ML}$  until the correct radius of the present day Sun was obtained. The other MLT parameters  $a$  and  $b$  are the flavor ML1 in Table 1.

Five such models were constructed, with values of  $\alpha_{ML}$  ranging from 1.6 to 5.2, as summarized in Table 2. The model A has  $\alpha_{ML} = 1.643$ ,  $g_{ML} = 1.0$ , and is typical of current solar models which use the Edington gray atmosphere as the outer boundary condition and conventional MLT (e.g., Schlattl, Weiss & Ludwig (1997)). This provides a baseline for comparison. Model D has  $\alpha_{ML} = 4.0$ , which is most consistent with hydrodynamic simulations.

Arnett, Meakin, & Young (2009) found that  $\alpha_{ML}$  was not constant, but depended upon the flow properties, and the equation of state. For solar models the surface con-

TABLE 2  
SOLAR MODELS WITH MLT

Model	$\alpha_{ML}$	$g_{ML}$	$R/R_{\odot}$	$L/L_{\odot}$	$r_{CZ}/R_{\odot}$	He <sub>surf</sub>	$v_m$ (km/s)
A	1.650	1.0	1.001	1.000	0.7169	0.2379	2.25
B	2.323	42.0	1.001	1.000	0.7172	0.2378	2.80
C	3.286	270.0	1.001	0.9997	0.7173	0.2377	3.05
D	4.000	595.0	1.000	0.9997	0.7168	0.2373	3.20
E	5.190	1,540.0	1.001	0.9998	0.7172	0.2377	3.40
Sun	...	...	1.000	1.000	$0.713 \pm 0.001$	0.24	3.20 <sup>a</sup>

<sup>a</sup>Inferred from the model data in Asplund, et al. (2005).

vection zone is deep, and changes little, so taking a constant  $\alpha_{ML}$  is an adequate approximation for this particular example. In MLT, the velocity obtained by a convective eddy is computed from the work done by the buoyancy force over a mixing length:

$$v_c^2 = \alpha_{ML}^2 g H_P \beta_T (\Delta \nabla) / 8, \quad (5)$$

where  $\beta_T$  is the compressibility,  $H_P$  the pressure scale height, and  $\Delta \nabla \equiv \nabla - \nabla_{ad}$  is the usual “super-adiabatic excess.” For a given convective luminosity, larger  $\alpha_{ML}$  implies larger velocities.

Shallow convection zones, having shorter distances for buoyant acceleration to work, will have smaller values of  $\alpha_{ML}$  and smaller velocity scales (Arnett, Meakin, & Young 2009). As the depth of the convection zone increases, the size of the largest eddies also rises, implying larger  $\alpha_{ML}$ . Such an increase will not continue indefinitely; more vigorous convection develops more violent dissipation. The value of  $\alpha_{ML}$  seems to “saturate” for very deep convection zones (Arnett, Meakin, & Young 2009; Meakin & Arnett 2009). The solar convection zone is 20 pressure scale heights deep, and has yet to be simulated for its full depth with resolution as high as used in Meakin & Arnett (2007b) or Stein & Nordlund (1998). Here we will examine the case in

which such saturation occurs at  $\alpha_{ML} \approx 4$ . This may be appropriate for the simulations of Nordlund and Stein (R. Stein, private communication) and those of Meakin & Arnett (2009), and is consistent with the insensitivity of the Stein & Nordlund (1998) simulations to the exact position of the lower boundary, which was deeper than this. Further analysis of this issue is in progress Meakin & Arnett (2009); 3D simulations for convective zones of depth 0.5 to 5 pressure scale heights seem consistent with this interpretation. The distribution of values for  $\alpha_{ML}$  in Table 2 covers this range.

Softer equations of state, such as in partial ionization zones or electron-positron pair zones, give less vigorous velocities, but do not change the qualitative picture (Arnett, Meakin, & Young 2009). The simulations of Porter & Woodward (2000), for an ideal gas equation of state, also seem to suggest that saturation may be beginning around  $\alpha_{ML} \approx 3$ , which is consistent.

Figure 1 shows the evolutionary tracks in the HR diagram, for each of the models (which differ only by the  $\alpha_{ML}$  and  $g_{ML}$  parameters). For each  $\alpha_{ML}$ , a value of  $g_{ML}$  is chosen which gives a reasonable radius for the present-day Sun. After passing the stellar birthline (deuterium burning,  $L \approx 10 L_{\odot}$ , see

Stahler & Palla (2004)), the tracks are very similar for all five models. However the increasing values of  $\alpha_{ML}$  imply increasing turbulent velocities (Eq. 5). Table 2 gives values of the radius ( $R/R_{\odot}$ ), luminosity ( $L/L_{\odot}$ ), the radius of the lower boundary of the convective zone ( $r_{CZ}/R_{\odot}$ ), the surface (convective zone) abundance of helium by mass fraction ( $\text{He}_{\text{surf}}$ ), and the maximum mean turbulent velocity in the convection zone ( $v_m$ ) in km/s. The increase in  $v_m$  with  $\alpha_{ML}$  is clear.

The models were adjusted to radius and luminosity of the present-day Sun to about one part in  $10^3$  or better, which is sufficient to show accurately the differential effects to be discussed here.

It is well known that, once a calibration of MLT parameters is done to fit the solar radius, paths in the HR diagram are little affected by which parameters were used (Pedersen, Vandenberg, & Irwin 1990; Salaris & Cassisi 2008). However, the variation of the velocity scale, although noticed by Pedersen, Vandenberg, & Irwin (1990) for example, has not been stressed. In Table 2 it is striking that only the velocity scale varies significantly with the variation of  $\alpha_{ML}$  and  $g_{ML}$  pairs constrained to fit the radius and luminosity of the present day Sun. This velocity scale is crucial for rates of entrainment, wave generation, and mass loss, and so may ultimately cause a change in the evolutionary behavior when such effects are correctly included. It will be argued below that this variation in the velocity scale has direct observational consequences (via line profiles and micro- and macro-turbulent velocities).

The values of the lower radius of the solar convection zone  $r_{CZ}$  and the surface helium abundance  $\text{He}_{\text{surf}}$  are slightly different from the values of the standard solar model. Part of the difference may be due to small errors in our stellar evolution code, which is not yet in its fully verified state. However the standard

solar model uses MLT and therefore ignores several significant aspects of convection: turbulent heating, flux of kinetic energy, and entrainment. These effects may move our models toward the inferred values from helioseismology. In any case the differential effects we discuss here are much larger, and unlikely to be affected by small modifications in the reference model. Notice that the predicted values of  $r_{CZ}$  and  $\text{He}_{\text{surf}}$  vary in only the fourth significant figure for models A through E while the velocity scale increases by more than 40 percent.

### 3. YREC and Garching Solar Models

Our solar models are in good agreement with YREC and Garching models, but not yet as close to either as they are to each other<sup>2</sup> In this paper we concentrate on the differences caused by changing MLT parameters and outer boundary conditions, rather than finding the absolute best standard solar model. Finding the absolute best solar model requires going beyond present formulations used in YREC and Garching codes (e.g., Michaud et al. (2004); Meakin & Arnett (2007b); Arnett, Meakin, & Young (2009)); we plan to address this in detail in future publications.

#### 3.1. Empirical Outer Boundaries

The Yale code (Demarque & Percy 1964; Guenther, Demarque, Kim & Pinsonneault 1992) uses as an outer boundary condition the empirically derived fit of Krishna Swamy (1966) to the  $T - \tau$  relation for the Sun,  $\epsilon$  Eridani, and Gmb 1830. Empirical fits have the flaw that they are suspect if extrapolated; these

<sup>2</sup>Our goal is to develop a software environment that allows modification of physical modules by logical switches, thus maintaining consistency between old and new implementations. We plan to persist until we have an option that removes even the small differences which remain for the standard solar model.

TABLE 3  
"BLOB SIZES" AND MIXING LENGTH

Model	$\alpha_{ML}$	$g_{ML}$	$\ell_b/H_P$	$\ell_b/\ell_m$
A	1.650	1.0	1.65	1.0
B	2.323	42.0	0.358	0.154
C	3.286	270.0	0.200	0.0608
D	4.000	595.0	0.164	0.0410
E	5.190	1,540.0	0.132	0.0255

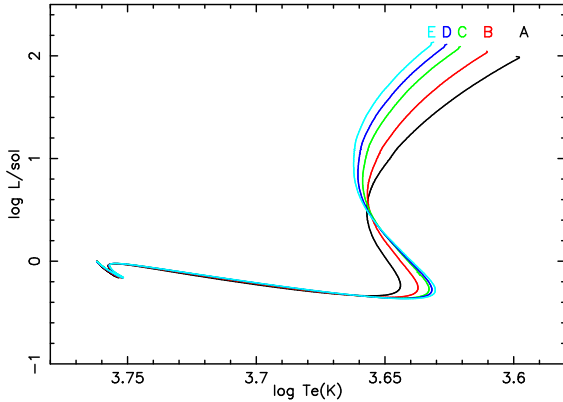


Fig. 1.— Solar models which differ only by the mixing length and the geometric factor, scaled to have the same radius. The trajectories in the HR diagram nearly overlay one another except on the Hayashi track, where they are poorly constrained. Note that the stellar birthline (Stahler & Palla 2004) lies near  $\log L/L_\odot \approx 1$ ; the more luminous parts of the tracks ignore accretion and so are not realistic.

stars are on the main sequence, and of G and K spectral type (G2V, K2V, and G8Vp, respectively). Gmb 1830 is a halo star of  $0.64M_\odot$  with a metallicity of about 0.1 of solar (Allende Prieto, et al. 2000), while  $\epsilon$  Eridani is a solar metallicity star of about  $0.85M_\odot$ . If applied to stars of the same stage of evolution and the same abundance, such empirical boundary conditions are at their best. Unfortunately the “calibration” approach may hide mistakes in the assumed physics.

### 3.2. Atmospheric Outer Boundaries

The Garching code (Schlatter 1996) was modified (Schlatter, Weiss & Ludwig 1997) to use synthetic atmospheres fitted to the interior solution at optical depth ( $\tau = 20$ ). In addition a spatially varying mixing length was employed to reproduce the pressure-temperature stratification calculated by 2D-hydrodynamic models (Freytag, Ludwig, & Steffen 1996). This involved the interpolation between an atmospheric value (Balmer-line fits gave  $\alpha_{at} = 0.5$ ) and an interior value ( $\alpha_{int} = 1.7$  to get the correct solar radius); see (Freytag, Ludwig, & Steffen 1996) for details. This approach can be extended with a library of hydrodynamic model atmospheres (and unlike the Yale approach, is not in principle limited to G stars). However, we find that our own 2D simulations, because of the pinning of vortices, do not mix material as

efficiently as 3D. For a given driving, 2D gives higher velocities to maintain the same convective luminosity (Asplund, et al. 2000; Meakin & Arnett 2007a,b). Further, 2D simulations have a different turbulent cascade and damping than 3D, which is related to this velocity difference. These issues need to be dealt with in making contact between actual convective velocities and observed line widths.

### 3.3. The Subphotospheric Region

How does changing the  $\alpha_{ML}$ — $g_{ML}$  pair affect the structure of the sub-photospheric layers? Figure 2 shows models A through E in the log pressure — log temperature plane. This may be directly compared with Fig. 1 in Schlattl, Weiss & Ludwig (1997). Model A is almost identical to their curve labeled “Eddington-approximation”, which used radiative diffusion and MLT with conventional parameters (essentially the same as model A,  $\alpha_{ML} \approx 1.7$  and  $g_{ML} = 1$ ). In contrast, model D, which also used the Eddington approximation but used MLT with  $\alpha_{ML} = 4.0$  and  $g_{ML} = 595.0$ , closely resembles their curves labeled “2D-hydro-model” and “1D-model-atmosphere”, and models C and E are similar. It appears that the significant point is not the choice of radiative diffusion versus radiative transfer, but rather the treatment of convection (VandenBerg, et al. 2008). The Yale group get hydrodynamics by empirical fitting to hydrodynamic observed atmospheres, the Garching group get hydrodynamics by a fit to their 2D hydrodynamic atmospheres, and we get hydrodynamics by analytic theory based on 3D simulations of convection.

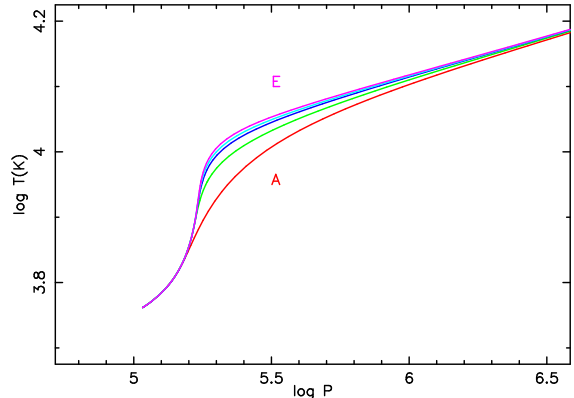


Fig. 2.— Structure of sub-photospheric regions with different choice of the  $\alpha_{ML}$  —  $g_{ML}$  pairs. Model A is the lowest curve, and models B, C, D and E are successively higher. Model A is similar to the “Eddington-approximation” case of Schlattl, Weiss & Ludwig (1997) while models C, D, and E are similar to their “2D-hydro-model” case.

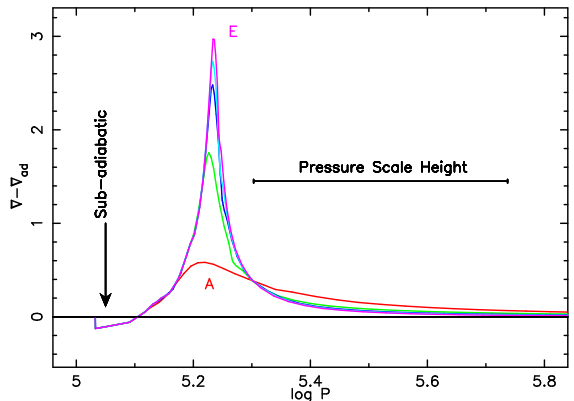


Fig. 3.— Structure of the super-adiabatic region (SAR), with  $\Delta\nabla = \nabla - \nabla_{ad}$  versus logarithm of pressure (dynes/cm<sup>2</sup>). The width of the SAR is much less than a pressure scale height; this may be compared with  $\ell_b/H_P$  in Table 2. The small blob size implied in models C, D, and E are consistent with the small width of the SAR, which is all we should expect without a 3D atmospheric model. Notice the small sub-adiabatic region just below the photosphere (the left of the graph, indicated by the arrow).



## 4. The SAR and Surface Velocities

### 4.1. The Geometric Factor $g_{ML}$

Although the traditional procedure for calibrating stellar convection is the variation of the parameter  $\alpha_{ML}$  to adjust the stellar radius keeping  $g_{ML}$  constant, this is not the most natural choice. It is  $g_{ML}$  that determines the radiative diffusion rate from “convective blobs”, and is most effective in the super adiabatic region (SAR). In the adiabatic regions, MLT gives an adiabatic gradient, so the choice of  $\alpha_{ML}$  is irrelevant to structure there. Historically, the reasonable choice — of forcing a one-parameter family by assuming constant values for all parameters except  $\alpha_{ML}$  — has obscured the physics. Simulations uncovered this mistake, with the indication that  $\alpha_{ML}$  is determined by the dissipation which is fed by the turbulent cascade, exactly as Kolmogorov (1941, 1962) suggested.

The geometric factor  $g_{ML}$  may be expressed in terms of a ratio of time to transit a mixing length to time for diffusion to remove the super-adiabatic excess from a “blob” (Kippenhahn & Weigert 1990). It is not well defined because of geometric vagueness about the “blob”; here we take it to be proportional to the inverse square of the ratio  $\ell_b/\ell_m$ , where  $\ell_b$  is the blob diameter and  $\ell_m$  the mixing length. This is a deviation from MLT, for which  $\ell_b \equiv \ell_m$ . With this identification we can compare the blob sizes for different  $\alpha_{ML}$ - $g_{ML}$  combinations given in Table 2.

This is shown in Table 3. Notice that for larger values of mixing length parameter  $\alpha_{ML}$ , the blob size becomes smaller, whether measured relative to a pressure scale height  $\ell_b/H_P = 1/\sqrt{g_{ML}}$  or relative to a mixing length  $\ell_b/\ell_m = 1/(\alpha_{ML}\sqrt{g_{ML}})$ . This means that, for acceptable solar pairs of  $\alpha_{ML}$ - $g_{ML}$ , larger values of the mixing length imply narrower and more intense superadiabatic regions to drive the convection. Larger values of mix-

ing length parameter  $\alpha_{ML}$  imply larger velocity scale (larger  $v_m$ ) as Table 2 shows. Thus, models A–E are a sequence having increasingly vigorous and narrowly restricted regions of convective driving (acceleration).

Figure 3 shows the structure of the SAR for models A through E. This may be compared to Fig. 2. of Schlattl, Weiss & Ludwig (1997). Again model A resembles their “Eddington-approximation” curve, and models C, D and E are similar to their “2D-hydro-model” and “1D-model-atmosphere” curves. Here  $\Delta\nabla \equiv \nabla - \nabla_a$  is plotted against logarithm of pressure (dynes/cm<sup>2</sup>).

Above the horizontal line  $\Delta\nabla = 0$ , buoyant forces accelerate the turbulent flow, while below the line we have buoyancy damping (deceleration; this region is barely visible at the left edge of the curve). According to MLT with the Schwarzschild criterion for convection, there should be no flow for  $\Delta\nabla \leq 0$ . The area above (under) the curve gives the net buoyant acceleration (deceleration). Clearly the deceleration, seen as the small depression near  $\log P = 5$ , is overcome by the much larger region of acceleration around  $\log P \approx 5.2$ , so that the Schwarzschild criterion gives incorrect results here. The area argument implied in Figure 3 is essentially the bulk Richardson number criterion (Fernando 1991; Meakin & Arnett 2007b), and is nonlocal. Therefore, because the pathological deceleration implied by use of the Schwarzschild criterion is incorrect, the velocities  $v_m$  given in Table 2 are directly related to those which produce solar line broadening.

### 4.2. Micro- and Macro-turbulence

Figure 4 shows the run of turbulent velocity as a function of optical depth for the five models, and for the Nordlund-Stein 3D hydrodynamic atmosphere quoted in Asplund, et al. (2005). The semi-empirical stellar atmosphere models of Fontenla et al. (2006) give

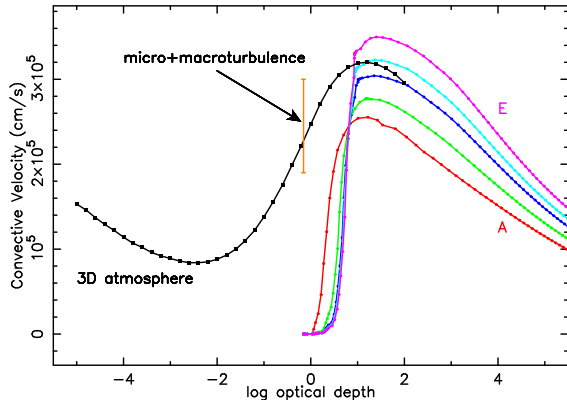


Fig. 4.— Convective velocities versus log optical depth for solar models which differ only by the mixing length and the geometric factor. The convective velocity changes while there are no other significant changes; standard mixing length theory with the Schwarzschild criterion was used. Case A had  $\alpha_{ML} = 1.643$  and the usual geometric factor,  $g_{ML} = 1$ . Case D ( $\alpha_{ML} = 4$  and  $g_{ML} = 595.0$ ) is the estimated value for saturation of the dissipation length for a solar convection zone of depth of 20 pressure scale heights. In MLT the velocity scale is not constrained physically, but only fixed by historical parameters (which are inconsistent with both 3D simulations and hydrodynamic theory). The 3D model atmosphere data from Asplund, et al. (2005) are dramatically different at small optical depth.

curves similar to those of Nordlund-Stein, but are not plotted to reduce crowding. The most striking feature in this figure is the difference between the low depth behavior of the models (an abrupt cliff at  $\tau \approx 1$ ), and the 3D-atmospheres (a gentler slope for lower  $\tau$ ). This is due to the use in the 1D models of the Schwarzschild criterion for convection, a local condition. A weakly-stable stratification cannot really hold back vigorous motion, as use of the local Schwarzschild criterion implies.

The micro- and macro-turbulent velocities,  $\zeta_{mi}$  and  $\zeta_{ma}$ , are parameters which were introduced long ago<sup>3</sup> to account for the embarrassment that, according to the Schwarzschild criterion, conventional solar atmospheres are *not convective* at the surface. Note that if  $\zeta = \sqrt{\zeta_{mi}^2 + \zeta_{ma}^2}$ , then  $1.9 \leq \zeta \leq 3.0$  km/s for the Sun (Cox 2000). This is indicated by the vertical bounded line in Figure 4. The connection between this  $\zeta$  and the actual turbulent velocity due to convection is not simple, involving line-formation, photon escape, and inhomogeneous stellar surface layers.

Fortunately, multi-dimensional hydrodynamic atmospheres (Asplund 2000; Nordlund & Stein 2000) do provide a spectacular fit to line shapes, with no free parameters, so we identify the convective velocities well below the photosphere (optical depth  $\tau \gtrsim 3$ ) in these simulations with those predicted by our hydro-dynamically consistent choice of mixing length parameter  $\alpha_{ML}$ . This means we are essentially matching different 3D simulations in the region of adiabatic convection, where they should give identical answers, and minimizing the sensitivity of the match to the complexities of atmospheric detail. Optical depth is sensitive to temperature (the opacity is  $\kappa \propto T^9$  here), so that the visible surface is a complex structure (see Fig. 24

<sup>3</sup>See Huang & Struve (1960) for an early review, in which  $\zeta$  is already a well established parameter.

in Stein & Nordlund (1998)). For example, a 10% fluctuation in temperature implies a change in 2.4 in the opacity. The optical depth of the photosphere occurs at different radii for different positions on the solar surface, so that fitting it with a single radius is difficult. At greater depths we expect the 3D atmospheres and the 1D models to agree, but near the surface it is not clear that the 3D and 1D definitions of optical depth are consistent.

Pressure should be a better coordinate for matching 3D results to a 1D model. Unlike the optical depth, the pressure is a weaker function of angular position on the solar surface. Hydrodynamic flow tends to smooth pressure variations, making the definition of a mean pressure-radius relation more meaningful. Figure 5 plots convective velocities versus log pressure for models A through E. We can see that the Asplund, et al. (2005) model smoothly joins onto model D.

Let us construct a simple model of the motion in this region to see how hydrodynamic arguments might give modifications to the purely hydrostatic boundary conditions used in models A through E. We will assume that the velocity is dominated by flow at the largest scales of turbulence. These scales contain most of the kinetic energy, and are least non-laminar. Convective motions are driven by the sinking of matter which is cooling due to transparency near the surface. This generates gravity waves in the near-surface region. We will approximate the large scale average of this motion by g-modes (Landau & Lifshitz (1959), see § 12) whose amplitude falls off exponentially with pressure scale height. This implied a scaling with position above an interface at radius  $r_0$ ,  $P(r) = P(r_0)v(r)/v(r_0)$ . Despite its extreme simplicity and harsh assumptions, this simple picture gives a significantly improved approximation to the behavior of the velocity in the photospheric re-

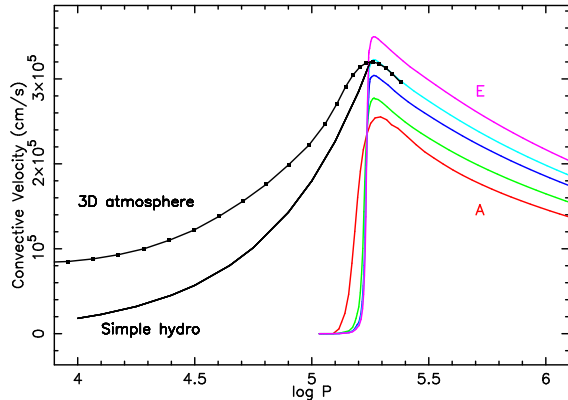


Fig. 5.— Convective velocities versus log pressure, for solar models and 3D hydrodynamic solar atmospheres. The atmospheres extend to lower pressure than the solar models (actually the atmospheres extend to higher pressure too, but these values were not in Table 1 of Asplund, et al. (2005)). It is clear that the 3D atmospheres would join smoothly onto solar model D for  $\alpha_{ML} = 4.0$  and  $g_{ML} = 595.0$ , as we would have predicted. The thin solid curve labeled “Simple hydro” represents a hydrodynamic extrapolation from the point of maximum convective velocity (see text). Replacing the MLT estimate (based on the Schwarzschild criterion and hydrostatic structure) with a physically motivated estimate gives a strikingly better agreement with both the 3D atmospheres and the empirical solar data.

gions. The thin black line labeled "Simple hydro" in Figure 5 represents such flow, fitted from the point of maximum convective velocity in model D. It captures the qualitative behavior far better than the conventional hydrostatic assumptions (shown as the steep "cliff" near  $\log P = 5.25$ ), and promises to do better as the complex physics of the photosphere is more faithfully represented (Stein & Nordlund 1998; Nordlund & Stein 2000).

This suggests that the photospheric velocity may be estimated by  $\zeta \approx 0.8 v_m$ , which predicts a connection between fitted line shapes and convective flow. Better physics for turbulent flow seems to be needed in 1D stellar atmospheres, and some 3D features are difficult to represent in 1D, such as inhomogeneity between upward and downward moving flows (Stein & Nordlund 1998; Nordlund & Stein 2000; Steffen, M. 2007). The 3D hydrodynamic atmospheres can provide insight into the correct mapping of realistic physics of a multi-modal region onto a 1D stellar model, and tighter constraints on  $\zeta$  for a given  $v_m$ . For Models A through E, this condition favors Model D.

Independent of any estimate of  $\zeta$ , our simulations and theory (Meakin & Arnett 2007b; Arnett, Meakin, & Young 2009) suggest from hydrodynamics alone that models C, D and E are most plausible, i.e.,  $\alpha_{ML}$  lies in the range of 3 to 5 because of enhancement of turbulent damping in deeply stratified convection regions ( $\alpha_{ML}$  "saturation"). This consistency is encouraging.

## 5. Summary

Insights from 3D compressible convection simulations and theory (Meakin & Arnett 2007b; Arnett, Meakin, & Young 2009) have been applied to sub-photospheric regions of solar models. Even within MLT, a dynamical

cally consistent velocity field (i.e., a consistent choice of  $\alpha_{ML}$  and an adjusted  $g_{ML}$ ), gives a better agreement with

1. empirical  $T(\tau)$  relations, and
2. 3D hydrodynamic models of stellar atmospheres.

Using the correct condition for mixing (the bulk Richardson number) implies that the 1D atmospheres should exhibit hydrodynamic flow. Further, simple hydrodynamic considerations (Press 1981; Press & Rybicki 1981) suggest g-mode waves will be generated and penetrate to the photosphere (these are generated by turbulent forcing from convection). We show that there is a connection between the predicted turbulent velocity scale and the observed (macro and micro)-turbulent velocities, which removes the embarrassment of non-convective surface regions predicted by 1D stellar atmosphere theory. As a bonus, we find that the observed macro- and micro-turbulence for the Sun can be used to fix the choice of  $g_{ML}$  (model D).

We may also have a resolution of an apparent contradiction. Atmospheric models of white dwarfs (Winget 2008; Bergeron et al. 1995), which have shallow convection zones, use MLT parameters (ML2:  $\alpha = 0.6$ , considerably smaller than used for the Sun), indicating less vigorous convection. Low mass eclipsing binaries (Stassun, et al. 2008; Morales, et al. 2008) are generally fit with  $\alpha \sim 1$  (again low convective efficiency), these models do *not* have shallow convection zones. In MLT there is no rationale for these differences. Use of Eq. 1 will give models having thin convection zones which agree with MLT models using small  $\alpha_{ML}$ , so we expect to reproduce the white dwarf results. For low mass stars, the surface temperatures will be lower than the solar value, so that the SAR should comprise more mass, i.e., we expect larger

$g_{ML}$  to be physically correct. Table 2 indicates that there is a trade off between  $\alpha_{ML}$  and  $g_{ML}$ : to compensate for lower  $g_{ML}$ ,  $\alpha$  must be lower, for the same radius. For a deep convection zone,  $\alpha_{ML}$  is fixed; then a stronger SAR (larger  $g_{ML}$ , and more inefficient convection) will give a larger radius. This is the sense of the discrepancy of the computed radii for low mass eclipsing binaries (Stassun, et al. 2008; Morales, et al. 2008), and we suggest that part of the discrepancy may be due to the convection algorithm used. Unfortunately, direct calculation of low mass dwarfs ( $M \approx 0.2M_{\odot}$ ) with  $\alpha_{ML} \approx 4$  exposes limitations in MLT: the SAR is forced upward into the photosphere, making 3D atmospheres a necessity for gaining insight into a plausible treatment in stellar models.

We have, in fact, sketched a way to eliminate astronomical calibration from stellar convection theory:

1. Adjust  $\alpha_{ML}$  from convection simulations. The mixing length is  $\ell_m = \alpha_{ML} H_P$  (where  $H_P$  is the pressure scale height), and equal to the depth of the convection up to  $4 H_P$ , and  $\alpha_{ML} \approx 4$  for deeper convection zones.
2. Adjust  $g_{ML}$  from 3D hydrodynamic atmosphere simulations, fitting the curve of super-adiabatic excess in the super-adiabatic region. This is more accurate, but equivalent to adjusting  $g_{ML}$  to reproduce a self-consistent SAR.

Notice that a fit to the present day solar radius is not logically necessary.

By seriously considering MLT, we have determined that no significant free parameters are left to adjust within the framework of the theory. We find that the choice of two characteristic lengths, *which are determined by the flow*, close the system: the turbulent dissipation length and the size of the super-adiabatic

region (SAR). Alternatively, the constraint that the observed micro- and macro-turbulent velocities agree with those predicted using the bulk Richardson criterion for surface convective mixing can be used instead of the SAR size.

MLT is still an incomplete theory, but it is suggestive that even modest changes toward a better physical interpretation, based upon 3D simulations and on a more complete turbulence theory, do give improvements in the models. MLT, as used here, may be derived from a more general turbulent kinetic energy equation by ignoring certain terms (Arnett, Meakin, & Young 2009). Some of the ignored terms are important, emphasizing that MLT is incomplete. However, the approach sketched above may be generalized, and inclusion of missing terms gives a convection theory that is nonlocal, time dependent, provides robust velocity estimates, and is based on simulations and terrestrial experiment, with no astronomical calibration. This more difficult theory will be presented in detail in future publications.

This work was supported in part by NSF Grant 0708871 and NASA Grant NNX08AH19G at the University of Arizona. We wish to thank Robert Stein for discussion of his unpublished work on turbulent damping in solar convection simulations, Robert Buchler for discussions on modeling time-dependent convection, and Martin Asplund for providing machine-readable copies of solar surface models.

## A. MLT Geometric Parameter

This analysis uses the formulation of Kippenhahn & Weigert (1990); see their discussion for more detail. In the mixing-length theory, there are two important conditions which involve radiative diffusion: luminosity conservation and blob cooling. The simple condition  $L = L(rad) + L(conv)$  is written as

$$(\nabla - \nabla_e)^{\frac{3}{2}} = \frac{8}{9}U(\nabla_r - \nabla), \quad (\text{A1})$$

which is identical to Eq. 7.15 of Kippenhahn & Weigert (1990). Here the subscripts on the  $\nabla$ 's denote  $e$  for mass element (the blob),  $a$  for adiabatic,  $r$  for radiative, and no subscript for the background (environment) value. The diffusive cooling of the blob implies

$$\nabla_e - \nabla_a = g_{ML}2U(\nabla - \nabla_e)^{\frac{1}{2}}, \quad (\text{A2})$$

which is identical to Eq. 7.14 of Kippenhahn & Weigert (1990), except for the introduction of a scaling factor  $g_{ML}$ . For  $g_{ML} \equiv 1$  we regain conventional MLT. Thus, the definition of  $U$  becomes

$$g_{ML}U = \frac{g_{ML}}{\ell^2} \left[ \frac{3acT^3}{\kappa\rho^2C_P} \left( \frac{8H_P}{g\beta_T} \right) \right], \quad (\text{A3})$$

which is their Eq. 7.12 with an extra factor  $g_{ML}$ , and our  $\beta_T$  is their  $\delta$ . If we define  $U^* = g_{ML}U$  and  $\zeta^2 = \nabla - \nabla_a + (U^*)^2$ , we may write

$$(\zeta - U^*)^3 + \frac{8}{9g_{ML}}U^*(\zeta^2 - (U^*)^2 - W) = 0, \quad (\text{A4})$$

which is Eq. 7.18 of Kippenhahn & Weigert (1990), except for the factor of  $g_{ML}$  in the denominator and the replacement of  $U$  by  $U^*$ . The same solution procedures may now be applied to solve for  $\zeta$  and hence  $\nabla$ . Any value of  $g_{ML}$  that is not excessively large or small (within a few powers of ten of unity) has no significant effect except in regions that are both convective and nonadiabatic.

An estimate of  $g_{ML}$  in terms of the size of a convective "element" or "blob" is given in Table 1 above, which we repeat here:  $g_{ML} = (\ell/\sqrt{3}r_b)^2$ , where  $r_b$  is the "blob" radius. In MLT,  $r_b \equiv \ell/\sqrt{3} \approx 0.577\ell$ , forcing two independent length scales,  $\ell$  and  $\sqrt{3}r_b$ , to be the same.

Adjustment of  $g_{ML}$  allows the super-adiabatic region to have the correct entropy jump, for any reasonable value of the mixing length parameter  $\alpha_{ML}$ ; that is,  $\alpha_{ML}$  may be chosen to be hydrodynamically consistent. This does *not* provide a consistent convective theory if other important effects, such as entrainment and wave generation, are ignored.

## REFERENCES

- Alexander, D. R., & Ferguson, J. W., 1994, *ApJ*, 437, 879
- Allende Prieto, C., Garcia Lopez, R. J., Lambert, D., & Ruiz Cobo, B., 2000, *ApJ*, 528, 885
- Arnett, D., Meakin, C., & Young, P. A., 2009, *ApJ*, 690, 1715
- Asplund, M., 2000, *A&A*, 359, 755
- Asplund, M., 2005, *ARA&A*, 43, 481
- Asplund, M., Grevesse, N., Sauval, A. J., Allende Prieto, C., & Kiselman, D., 2005, *A&A*, 435, 339
- Asplund, M., Ludwig, H.-G., Nordlund, Å., Stein, R. F., 2000, *A&A*, 359, 669
- Bahcall, J. N., 1989, *Neutrino Astrophysics*, Cambridge University Press, Cambridge
- Bahcall, J. N. & Pinsonneault, M. H., 2004, *Phys. Rev. Lett.*, 92, 121301
- Bahcall, J. N., Serenelli, A. M., & Pinsonneault, M., 2004, *ApJ*, 614, 464
- Balbus, S. A., & Hawley, J. F., 1998, *Rev. Mod. Phys.*, 70, 1
- Balbus, S., 2008, arXiv:0809.2883
- Bergeron, P., Saumon, D., and Wesemael, F., 1995, *ApJ*, 443, 764
- Böhm-Vitense, E., 1958, *ZAp*, 46, 108
- Clayton, D. D. 1983, *Principles of Stellar Evolution and Nucleosynthesis*, University of Chicago Press, Chicago
- Cox, A., ed., *Allen's Astrophysical Quantities*, 4th Ed., AIP, Springer-Verlag, New York
- Cox, J. P., 1968, *Principles of Stellar Structure*, in two volumes, Gordon & Breach, New York
- Demarque, P., & Percy, J. R., 1964, *ApJ*, 140, 541
- Fernando, H. J. S., 1991, *Ann. Rev. Fluid Mech.*, 347, 197
- Fontenla, J. M., Avrett, E., Thuillier, G., & Harder, J., 2006, *ApJ*, 639, 441
- Freytag, B., Ludwig, H.-G., & Steffen, M., 1996, *A&A*, 313, 497
- Grevesse, N. & Sauval, A. J., 1998, *Space Science Reviews*, 85, 161
- Guenther, D. B., Demarque, P., Kim, Y.-C., & Pinsonneault, M. H., 1992, *ApJ*, 387, 372
- Hansen, C. J., & Kawaler, S. D., 1994, *Stellar Interiors*, Springer-Verlag
- Huang, S., & Struve, O., 1960, in *Stellar Atmospheres*, ed. J. Greenstein, University of Chicago Press, p. 321
- Iglesias, C. & Rogers, F. J. 1996, *ApJ*, 464, 943
- Kippenhahn, R. & Weigert, A. 1990, *Stellar Structure and Evolution*, Springer-Verlag
- Kolmogorov, A. N., 1941, *Dokl. Akad. Nauk SSSR*, 30, 299
- Kolmogorov, A. N., 1962, *J. Fluid Mech.*, 13, 82
- Krishna Swamy, K. S., 1966, *ApJ*, 145, 174
- Landau, L. D. & Lifshitz, E. M., 1959, *Fluid Mechanics*, Pergamon Press, London
- Meakin, C., & Arnett, D., 2007a, *ApJ*, 665, 690.
- Meakin, C., & Arnett, D., 2007b, *ApJ*, 667, 448.

- Meakin, C., & Arnett, D., 2009, in preparation.
- Michaud, G., Richard, O., Richer, J., & Vandenberg, D. A. 2004, *ApJ*, 606, 452
- Morales, J. C., Ribas, I., Jordi, C., Torres, G., Gallardo, J., Guinan, E., Charbonneau, D., Wolf, M., Latham, D. W., Anglada-Escude, G., Bradstreet, D. H., Everett, M. E., O'Donovan, F. T., Maudushev, G., Mathieu, R. D., 2008, arXiv:0810.1541v1
- Nordlund, A., & Stein, R., 2000, *The Impact of Large-Scale Surveys on Pulsating Star Research*, ASP Conf. Series, 203, 362
- Pedersen, B. B., Vandenberg, D. A., & Irwin, A. W., 1990, *ApJ*, 352, 279
- Porter, D. H., & Woodward, P. R., 2000, *ApJS*, 127, 159
- Press, W. H. 1981, *ApJ*, 245, 286
- Press, W. H. & Rybicki, G. 1981, *ApJ*, 248, 751
- Rauscher, T., & Thielemann, K.-F., 2000, *Atomic Data Nuclear Data Tables*, 75, 1
- Rodgers, F. J., Swenson, F. J., & Iglesias, C. A., 1996, *ApJ*, 456, 902
- Salaris, M. & Cassisi, S., 2008, *A&A*, in press
- Schlattl, H., 1996, Diploma Thesis, Tech. Univ. Munich
- Schlattl, H., 2002, *A&A*, 395, 85
- Schlattl, H., Weiss, A., & Ludwig, H.-G., 1997, *A&A*, 322, 646
- Stahler, S. W. & Palla, F., 2004, *The Formation of Stars*, WILEY-VCH Verlag GmbH & Co. Weinheim, Germany
- Stassun, K. G., Hebb, L., López-Morales, M., and Prša, A., 2008, in *Ages of Stars*, IAU Symposium 258, E. E. Mamajek and D. Soderblom, eds., Cambridge University Press
- Steffen, M., in *Convection in Astrophysics*, ed. F. Kupke, I. Roxburgh, and K. Chan, IAU Symp. 239, Cambridge University Press, 36
- Stein, R. F., and Nordlund, Å., 1998, *ApJ*, 499, 914
- Tassoul, M., Fontaine, G., and Winget, D. E., 1990, *ApJS*, 72, 335
- Thoul, A. A., Bahcall, J. N., & Loeb, A. 1994, *ApJ*, 421, 828
- Timmes, F. X. & Swesty, F. D. 2000, *ApJS*, 126, 501
- Vandenberg, D. A., Edvardsson, B., Eriksson, K., and Gustafsson, B., 2008, *ApJ*, 675, 746
- Vitense, E., 1953, *ZAp*, 32, 135
- Winget, D. E., and Kepler, S. O., 2008, *ARA&A*, 46, 157